九州大学学術情報リポジトリ
Kyushu University Institutional Repository

Second Law-Based Assessment of Combined Cycle Power Plant

Madan, Komal
Mechanical and Automation Engineering Dept., Indira Gandhi Delhi Technical University for Women

Omendra Kumar Singh
Mechanical and Automation Engineering Dept., Indira Gandhi Delhi Technical University for Women

https://doi.org/10.5109/6781093

出版情報：Evergreen. 10 (1), pp.356-365, 2023-03. 九州大学グリーンテクノロジー研究教育センター
バージョン：
権利関係：Creative Commons Attribution-NonCommercial 4.0 International

Second Law-Based Assessment of Combined Cycle Power Plant

Komal Madan[1,*], Omendra Kumar Singh[1,]

[1] Mechanical and Automation Engineering Dept., Indira Gandhi Delhi Technical University for Women, Delhi, India

*Author to whom correspondence should be addressed:
E-mail: komal55_90@yahoo.co.in

(Received July 12, 2022; Revised January 24, 2023; accepted January 24, 2023).

Abstract- Energy is the main driving force to raise the economy of a nation. The demand for energy grows proportionally with the population of the country. The combined cycle technology is one of the most efficient and widely used technologies for power generation these days if natural gas is utilized as fuel. To meet the ever-growing electric energy demand with decreasing fossil fuel resources, it is necessary to further improve the performances of power generation systems. This can be done either by installing new plants with improved technology or by reducing losses within the existing plants. The present work investigates the thermodynamic performance of the existing Brayton-Rankine power plant currently in operation in India with actual operating data. Energy and exergy analyses of the said plant have been carried out through a computational model coded in MATLAB taking into consideration the important aspect of identifying the places and components of maximum thermodynamic losses which is the originality in the present work. Using the combustion energy of the fuel, which is 759.290 MW, the theoretical value of net power generated, overall thermal efficiency and exergetic efficiency of the plant is estimated to be 317.381 MW, 41.79 %, and 40.19 % respectively. The combustion chambers of the two gas turbines are turned out to be the most irreversible component with the maximum percentage of exergy destruction (14.9 %).

Keywords: Combined cycle power generation plant; Simulation model; Parametric analysis; Fuel temperature; Exergy destruction

1. Introduction

Energy is the main driving force to raise the economy of a nation. The demand for energy grows proportionally with the population of the country. Therefore, fossil fuels will dominate the power sector and contribute 85% of the world's power generation for the next 30 years, despite causing greenhouse gas emissions into the environment. Combined cycle based-power plants are among the most reasonable electric energy generation plants that combine two different conventional power generating cycles, namely the gas Brayton cycle as topping cycle and the steam Rankine cycle as bottoming cycle connected by a heat recovery steam generator (HRSG). This power cycle is more preferred compared to the individual cycle due to its high efficiency, low emissions, and operational flexibility. Aiming to fulfill the future energy demands or to make any attempt of modification, it is necessary to conduct a comprehensive thermodynamic assessment of the considered system to calculate the performances of each of the component of the system and that of the whole system. The energy balance gives no information regarding the internal losses taking place in a component. The shortcoming of the Ist law is overcome by the 2nd law-based analysis, i.e., the exergy analysis which is used to quantify the true performance of various thermal systems. The said analysis has been used to evaluate, optimize, and modify a broad spectrum of thermal systems and processes, such as thermal power plant [1) 2)]. Refrigeration and air conditioning system [3-6)], solar thermal system [7-9)], and organic Rankine cycle [10)].

2. Research background

The combined cycle power plant (CCPP) is a complex system, and it is not possible to truly analyze its operation with assumed operating conditions and data. An extensive research was done time-to-time by various researchers on these power plant to augment its performance through energetic and exergetic approach [11-15)]. Cihan et al., [16)] evaluated the energy and exergy analysis of a 1000 MW capacity natural gas based-CCPP situated at Luleburgaz in Turkey to analyze the performance and complexities of the existing power

plant. Ibrahim et al., [17] studied the performance of CC with and without regenerative gas turbine configurations to examine the effects of ambient temperature and compression ratio by developing a simulating code in MATLAB10 software. Ameri et al., [18] evaluated the irreversibilities of each component of the Neka power plant through the 2nd law-based analysis and studied the effect of duct burner on steam turbo-generator output power. Ersayin and Ozgener, [19] investigated the thermodynamic performance of a CCPP using the operating data and by applying first and second law equations. They also conducted the parametric analysis by studying the influence of outside temperature on the efficiency of the system. The results of energy and exergy efficiencies came out to be 56 % and 50.04 % respectively. The operating performance of these power generation systems depends upon components behavior that varies due to change in the design parameters. Hence, parametric analysis of these plants is imperative with any modification in the existing component [20-22]. Khaliq and Kaushik, [23] developed and derived the second law-based equations to analyze the Brayton-Rankine power cycle with reheat and investigate the effect of different design parameters on the output performance of the system. Aliyu et al., [20] performed the thermodynamic assessment of the steam Rankine cycle of triple pressure CCPP with reheat using the design data to identify the losses occurring within each component and strengthen the overall performance of the system. For analyzing the impact of parameters of the steam cycle on the performance of overall CC, parametric analysis was done. They outlined that the maximum exergy destruction in the steam cycle was found to occur in stack followed by HRSG, turbine, and condenser.

The present research work is motivated by the fact that the majority of the thermal power plants in India are quite old and operate with poor efficiency. Replacing these plants with modern and advanced technology would require heavy investment. In order to find ways to improve their efficiency with low capital investment, it is necessary to examine the quantity and quality of the waste heat. In view of this, thermodynamic performance analysis is carried out using the operating and design data of existing natural gas-fired CCPP located in India to identify the components where maximum thermodynamic losses are occurring so as to be able to make modifications because the places of maximum destruction are the places which have the maximum prospects for improvement. Also, the effect of ambient temperature, fuel temperature, and pinch point temperature were studied to meet the demand in peak load conditions. The objectives of the proposed work are relevant for further advancement in power plant technology.

3. Research methods

3.1 System description

The existing power plant considered in the present work, is National Capital Power Station, NTPC, Dadri which is a natural gas fuelled CCPP of 817 MW capacity and consists of two units. The operating and design data of its No. 1 unit were collected from the control room in the month of October, 2017 and are presented in Tables 1-2. The simplified diagram of the No. 1 unit is presented in Fig.1. The considered unit of the power plant consists of a topping cycle of two Gas Turbine engines of 131 MW capacity each and a bottoming cycle of one Steam Turbine (comprising of HP stage and LP stage) of 146.5 MW capacity.

In the topping cycle, there are two gas turbine units. Each unit comprises of a compressor, a fuel combustor, and a gas turbine. The fuel used in the two gas turbine units is natural gas with volumetric composition as follows, 94 % CH_4, 4 % C_2H_6, 1.2% C_3H_8, 0.78 % C_4H_{10}, 0.02 % N_2. As shown in Fig.1, the atmospheric air is sucked (state points g_1 and g_6) by the compressors of the two gas turbine engines and compressed to high pressure (state points g_2 and g_7). The compressed air from the compressors goes into the combustors of the gas turbine engines to burn fuel entering at state points f_1 and f_2. The product gases so formed in the combustion chambers expand in the two gas turbines (state points g_3 and g_8) to produce shaft work. A fraction of the mechanical work developed by a gas turbine is utilized to run the compressor of that unit. The high temperature exhaust gases exiting from the two turbines (state points g_4 and g_9) enter into two HRSGs to generate superheated steam.

The two dual-pressure HRSGs connect the two top cycles with the bottom cycle and utilize most of the heat of the gases leaving the two gas turbine units to generate superheated steam (HP and LP) and then discharge the gases containing low-grade heat into the environment through the stack. This low-grade heat of the exhaust gases is wasted into the environment. In addition to the two HRSGs, there are three Boiler Feed Water Pumps (both HP and LP), a Condenser, three Condensate Extraction Pumps (CEP), two Condenser Preheaters (CPH), a Deaerator, and a Cooling Tower in the bottoming cycle.

Each of the dual pressure HRSGs consists of three heat exchanger sections namely economizer, evaporator, and superheater. The two Feed Water Pumps namely, High-Pressure Boiler Feed Water Pump (HPBFW Pump) and Low-Pressure Boiler Feed Water Pump (LPBFW Pump) supply feed water to HP and LP economizers respectively. In economizer, feed water is heated to its saturation point and then flows into the steam drums. The heated feed water is evaporated in the evaporating loop of the HRSGs at constant temperature and pressure and flows back to the steam drums where water and saturated steam are separated from each other. The

saturated steam is then fed into the superheater loop to superheat the steam to the desired temperatures. The high-pressure superheated steam (state points 16 and 17) is fed into the HP turbine (state point 1) and the low-pressure superheated steam (state points 22 and 23) is fed into the LP turbine (state point 3). The steam expands in the two turbines and develop power in the bottoming cycle. A part of the steam (Approximately 12%) leaving the HP turbine flows into the deaerator (state point 25) and the rest into the LP turbine (state point 24). The low-pressure and temperature steam exiting from the LP turbine (state point 4) flows into the condenser where it is condensed into the liquid condensate by rejecting its latent heat of condensation to the cooling water and is drained into the hot well. The condensate from the hot well (state point 5) is pumped to the deaerator by the CEP through the condensate preheater and the cycle is completed. The condensate preheater heats the condensate coming from the Hot well. In the considered system, vacuum deaeration is preferred to avoid the additional cost of the heat exchanger required by heating feed water within the feed water tank using the heating steam. The exhaust gases leaving the HRSGs (state points g_5 and g_{10}) flow out into the atmosphere through the stack. The stack losses are low with a dual-pressure HRSG. However, the condenser cooling water requirement and hence, the power consumed by the condenser cooling water circulation pumps are increased due to the additional steam flowing into the condenser from the LP turbine.

3.2 System assumptions and modelling

For thermodynamic analysis of the system, following assumptions are taken into account:

- All of its components are presumed to be control volume under steady state for mass, energy, and exergy analysis.
- Neglected change in kinetic and potential energies and exergies of the component.
- No thermal energy loss from water and steam pipes.
- In the condenser, the heat loss to the surrounding is assumed to be negligibly small due to its perfectly insulated outside surface and small temperature variation between the inside and the surrounding atmosphere.
- However, the heat losses to the surrounding from the surfaces of the two HRSGs and Deaerator are substantial and quite considerable because of high temperature variation between the inside of these heat exchangers and the surrounding atmosphere. This heat loss is taken from the actual data collected at the plant site at the time of data collection.
- There is no pressure loss in the components and the connected piping.
- All gases are ideal gases.
- The combustion of fuel takes place adiabatically and at constant pressure.
- The expansion process in the gas turbines and the compression process in the compressors are reversible adiabatic or isentropic processes.
- In the topping cycle, the working fluid is the product of combustion while that in the bottoming cycle is water/steam.

Table 1. Operating data of CCPP.

Input data	**Value**	**Units**
Ambient Temperature	307.15	K
Ambient Pressure	100900	Pa
Relative Humidity	33	%
Compressor Pressure Ratio of GT 1/GT 2	10.2	-
Isentropic Efficiency of Compressor GT1/GT2	88	%
Fuel Consumption at ambient conditions of GT 1	40444	m^3/h
Fuel Consumption at ambient conditions of GT 2	40861	m^3/h
Fuel Inlet Temperature for Combustor 1 and 2	309.15	K
Fuel Inlet Pressure for Combustor 1 and 2	2560325	Pa
Power produced by two gas turbines	100.36/103.50	MW
Power produced by steam turbine	110	MW
Maximum Temperature of topping cycle 1	1327.15	K
Maximum Temperature of topping cycle 2	1352.15	K
Isentropic Efficiency of Gas Turbine GT1/GT2	77	%
Gas Turbine pressure ratio GT1/GT2	9.7382	-
The inlet temperature of Cooling Water into the condenser	30	°C
The exit temperature of Cooling Water from the condenser	39	°C

Table 2. Steam cycle data at different state points

State Points	$\hat{m}$ **(kg/s)**	P **(MPa)**	T **(K)**
1	115.90	5.9613	779.70
2	115.90	0.6553	479.65
3	161.12	0.6260	480.59
4	161.12	0.0100	318.96

5	161.12	0.0100	317.85
6	161.12	1.5813	317.71
7	80.90	1.5813	317.71
8	80.30	1.5813	317.71
9	80.90	0.8523	361.15
10	80.30	0.8603	362.55
11	161.20	0.8563	360.25
12	115.90	0.4623	407.15
13	115.90	11.9913	407.19
14	58.10	11.9913	407.19
15	57.80	11.9913	407.19
16	58.10	6.1713	779.70
17	57.80	5.7513	779.70
18	59.10	0.4623	407.15
19	59.10	1.4163	408.68
20	29.80	1.4163	408.68
21	29.30	1.4163	408.68
22	29.80	0.6393	483.05
23	29.30	0.6493	483.05
24	59.10	0.6443	483.05
25	13.87	0.6553	479.65

The actual composition of air by volume can be calculated at the ambient conditions using the procedure described in [24] and is obtained as: 20.55% O_2, 76.61 % N_2, 1.89 % H_2O, 0.030806 % CO_2, 0.92 % Ar. Using the inlet temperatures of the gas turbines (GT1 & GT2) given in Table 1, the excess air required is found to be 3.509 and 3.381 times of theoretical air for units 1 and 2 respectively. Therefore, the combustion of 1 kilo mol of fuel can be written as

$$\overbrace{0.94CH_4+0.04C_2H_6+0.012C_3H_8+0.0078C_4H_{10}+0.0002N_2}^{Fuel}+\overbrace{2.131*(O_2+3.7279N_2+0.0919H_2O+0.001498CO_2+0.0447Ar)*3.509}^{Air}\longrightarrow\overbrace{1.09838CO_2+2.7732H_2O+5.3307O_2+27.816N_2+0.33403Ar}^{Gas} \quad (1)$$

The Air to fuel ratio by mass may be expressed as

$$\left(A/F\right)_{mass}=\frac{n_a\times M_a}{n_f\times M_f} \quad (2)$$

The rate of heat generation by fuel $\hat{E}_f$ in kJ/kmol of fuel is estimated from [25]. The specific molar heat capacity $\dot{C}_{p,i}$ (kJ/kmol-K) for the fuel and other gases are calculated from [26].The sensible heat of enthalpy (kJ/s) may be expressed as:

$$\sum_{i=1}^{m}\dot{n}_i*\int_{T0}^{T}\dot{C}_{p,i}dT \quad (3)$$

Where, 'i' denotes the number of component, $'\dot{n}_i'$ is the molar flow rate of the component (kmol/s), and $\int_{T0}^{T}\dot{C}_{p,i}dT$ is the molar physical enthalpy (kJ/kmol) of the component.

Applying steady-state energy equation under control volume condition, the mass $(\hat{m})$ energy $(\hat{E})$, and exergy (ψ) conservation can be defined as [26]

$$\sum\hat{m}_{in}=\sum\hat{m}_{ex} \quad (4)$$

$$\hat{E}_Q-\hat{E}_W=\sum\hat{m}_{ex}h_{ex}-\sum\hat{m}_{in}h_{in} \quad (5)$$

$$\sum\hat{m}_{in}\psi_{in}+\hat{X}_Q=\sum\hat{m}_{ex}\psi_{ex}+\hat{X}_W+\hat{X}_D \quad (6)$$

Where subscript 'in' and 'ex' defines the inlet and exit conditions of fluid, h is the specific enthalpy.

The rate of flow of exergy due to heat transfer ($\hat{Q}_i$) at temperature (T) and ambient temperature (T_o) and that due to work transfer ($\hat{W}$) can be defined as

$$\hat{X}_Q=(1-\frac{T_0}{T})\hat{Q}_i \quad (7)$$

$$\hat{X}_W=\hat{W} \quad (8)$$

The total specific exergy (ψ_{tot}) can be written as

$$\psi_{tot}=\psi_{phy}+\psi_{ch} \quad (9)$$

The physical (ψ_{phy}) and chemical exergy (ψ_{ch}) of air, water/steam, a mixture of gases, and fuel $(\hat{X}_f)$ can be evaluated from [14].

3.3 Performance parameters

The combined cycle power output is given by

$$\hat{P}_{ECC}=\hat{P}_{TC1}+\hat{P}_{TC2}+\hat{P}_{BC} \quad (10)$$

The combined cycle thermal efficiency is given by

$$\eta_{ECC}=\frac{\hat{P}_{ECC}}{\hat{E}_f} \quad (11)$$

The combined cycle exergy efficiency is given by

$$\eta_{ex}=\frac{\hat{P}_{ECC}}{\hat{X}_f} \quad (12)$$

The combined cycle exergy destruction rate is given by

$$\hat{X}_{D,ECC} = \hat{X}_{D,CA} + \hat{X}_{D,Comb} + \hat{X}_{D,GT} + \hat{X}_{D,HRSG} + \hat{X}_{HPST} + \hat{X}_{LPST} + \hat{X}_{D,CEP} + \hat{X}_{D,Dea} + \hat{X}_{D,CPH} + \hat{X}_{D,CON} + \hat{X}_{D,stack} \quad (13)$$

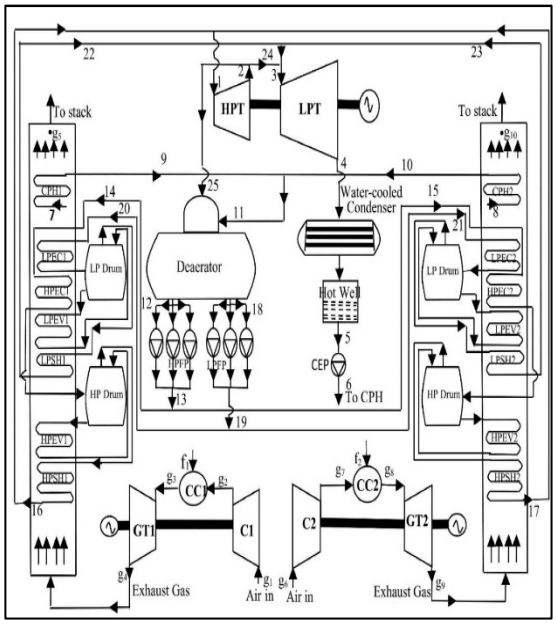

Fig. 1. Simplified diagram of existing Brayton-Rankine power plant

4. Results and discussions

The results obtained from the 2nd law based thermodynamic performance analysis and parametric study of the considered unit of the operational National Capital Power Station, NTPC, Dadri using the actual operating data, as given in Tables 1-2 are presented below. Fig. 2. presents and compares the theoretically calculated values of the net power output of the existing CCPP under consideration with the actual data of the plant. The deviation of the theoretical results from the actual operating data of the plant is not very much appreciable and is due to a number of assumptions made in the analysis such as isentropic processes of expansion in the turbines and compression in compressors, steady-state operation of the plant components, isentropic pumping of feed water by pumps, negligible pressure losses, etc. In actual practice, the operating conditions are not as per the assumptions made. However, the deviation is well within the specified limit indicating the accuracy of the analysis conducted in the proposed work. Due to the accuracy of the analysis, the exergy destruction rate occurring in different elements of the plant will be truly obtained with the help of which, it will be possible to identify the components with maximum thermodynamic losses so that attention may be focused on such components from the perspective of plant modifications. Using the combustion energy of the fuel, which is 759.290 MW, the theoretical value of net power produced is estimated to be 317.381 MW which is very close to the actual value (314.06 MW) of the power output indicating the accuracy and authenticity of the present analysis. The overall thermal efficiency of the plant is estimated to be 41.79 %. Fig. 3. depicts the energy losses taking place in various components of the combined cycle. It can be seen from Fig 3. that the maximum energy loss is occurring in the condenser (50.86 %) accompanied by HRSGs (3.71 %) and the deaerator (.00158 %). However, the energy, which is lost in the condenser, is the low-grade heat energy that cannot be utilized any longer for power production in the steam bottoming cycle. It is for this reason that this energy has to be dissipated to the cooling water being circulated through the condenser tubes.

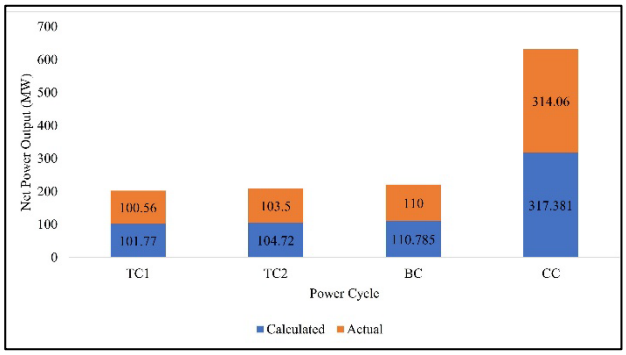

Fig. 2. Comparison of actual and theoretical results of power plant

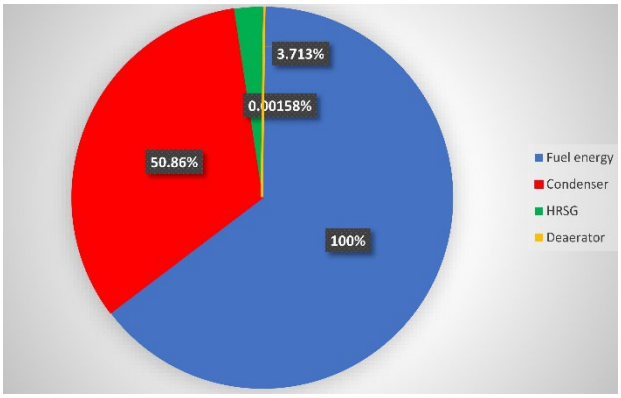

Fig. 3. Energy loss in components of CCPP relative to the combustion energy input.

Referring to the diagram shown in Fig. 1. and applying the equations at different state points of the existing CCPP, the outcomes of the exergy analysis obtained are displayed in Tables 4-5. The total exergy content of the fuel for both the gas turbine units taken together is estimated to be 783.280 MW. The rate of exergy destruction and exergetic efficiency of the CCPP is quantified to be 393.995 MW and 40.19 % respectively. Table 6. presents irreversibilities occurring in each

component of the power plant. It is identified that the combustion chamber is the most irreversible component with the maximum percentage of exergy destruction (14.96 %) followed by the stack (11.84 %), the HRSGs (11.7 %), the steam turbine (7.74 %) and the two gas turbines (5.27 %). The main cause of irreversibility in the two combustion chambers is the chemical reactions taking place among the fuel and the air [27]. In the present analysis, the exergy loss from the stack is found to be around 92.749 MW which is due to a large amount of energy discharged out together with the flue gases at moderate temperature, therefore containing a lot of exergy.

Table 4. Exergy analysis of gas Brayton cycle at P_0=100900 Pa and T_0=307.15 K.

State Points	P (kPa)	T (K)	$\dot{n}$ (kmol/s)	H (kW)	X kJ/s)
g1	100.9	307.15	16.047	0	0
g2	1029.2	635.81	16.047	158990	147920
g3	1013.7	1327.15	15.937	555240	439750
g4	104.1	870.29	15.937	293670	162980
g5	101	373.15	15.937	32783	46307
g6	100.9	307.15	15.619	0	0
g7	1029.2	635.81	15.619	154760	143970
g8	1013.7	1352.15	16.084	555520	455050
g9	104.1	886.68	16.084	295200	170250
g10	101	369.15	16.084	30014	46552

Table 5. Exergy analysis of steam Rankine cycle at P_0=100900 Pa and T_0=307.15 K.

State Points	$\hat{m}$ (kg/s)	P (MPa)	T (K)	ψ (kJ/kg)	$\dot{X}$ (kJ/s)
1	115.90	5.9613	779.70	1338.920	155180.9
2	115.90	0.6553	479.65	744.1748	86249.86
3	161.12	0.6260	480.59	738.6446	119013.4
4	161.12	0.0100	318.96	90.36107	14559.34
5	161.12	0.0100	317.85	0.679235	109.4411
6	161.12	1.5813	317.71	2.237010	360.4360
7	80.90	1.5813	317.71	2.237010	180.9741
8	80.30	1.5813	317.71	2.237010	179.6319
9	80.90	0.8523	361.15	18.58491	1503.519
10	80.30	0.8603	362.55	19.49808	1565.695
11	161.20	0.8563	360.25	18.03238	2906.820
12	115.90	0.4623	407.15	57.06715	6614.083
13	115.90	11.991	407.19	68.31199	7917.359
14	58.10	11.991	407.19	68.31199	3968.926
15	57.80	11.991	407.19	68.31199	3948.433
16	58.10	6.1713	779.70	1342.571	78003.38
17	57.80	5.7513	779.70	1334.954	77160.36
18	59.10	0.4623	407.15	57.06715	3372.669
19	59.10	1.4163	408.68	59.59959	3522.335
20	29.80	1.4163	408.68	59.59959	1776.068
21	29.30	1.4163	408.68	59.59959	1746.268
22	29.80	0.6393	483.05	743.2217	22148.01
23	29.30	0.6493	483.05	745.3018	21837.34
24	59.10	0.6443	483.05	744.3118	43988.83
25	13.87	0.6553	479.65	744.1748	10326.17

4.1 Effect of different operating variables

The thermodynamic model of the existing CCPP is validated by the fact that the theoretical results of the power produced by the gas and steam turbines match well with their actual outputs. This validates the simulation model of the plant developed in MATLAB in the present work. The same simulation model can, therefore, be used to investigate the effects of different operating variables, namely, compressor inlet temperature, fuel temperature, and pinch point temperature on the output characteristic of the existing system.

The compressor inlet temperature has been found to have a substantial effect on the performance of the existing power plant. The compressor inlet temperature is varied in the present research from 296 K to 309 K because of unpredictable atmospheric conditions in India. Fig. 4. shows the effect of compressor inlet temperature on the net power output and overall thermal efficiency of the said system. It is clear from the graph that both variables increase with decrease in the compressor inlet air temperature. This is because, with a drop in inlet air temperature, the density of air increases and hence its mass flow rate also increases. Moreover, the compressor work is directly related to the inlet air temperature which increases with a decrease in inlet temperature.

Table 6. Irreversibilities in various components of the plant

Components	Exergy destruction rate	
	MW	%
Air compressors	21.853	2.76
Combustors	118.199	14.96
Gas Turbines	41.33	5.27
HRSG	91.859	11.72
Steam Turbine	61.133	7.74
Condenser	12.349	1.39
Pumps and deaerator	3.742	0.474
Stack	92.759	11.84

Fuel temperature is another crucial parameter to study from the aspect of fuel saving and therefore the cost of power generation. Keeping all other parameters same, the fuel consumption rate is inversely correlated to the temperature of the fuel entering the combustion space. If fuel is supplied to the combustion chamber at a higher temperature, less amount of heat will be required to be generated for the same turbine inlet temperature, thereby saving in the rate of fuel consumption for the same power developed. In the present analysis, the temperature of incoming fuel is varied from 309.15 K to 327.15 K and its effects on the net power output and the overall thermal efficiency of the said cycle are plotted in Fig. 5. It is seen from Fig. 5. that a rise in fuel inlet temperature, decreases the power output of the plant. This is because, at higher fuel temperature, the density of the fuel decreases and therefore, for the same volumetric flow rate of the fuel, its mass flow rate would reduce thereby developing less power for the same volumetric flow rate of the fuel. However, the reverse effect of fuel inlet temperature is observed on the overall thermal efficiency of the considered plant. Fig. 5. also depicts that a rise in the fuel temperature increases the efficiency for the same volumetric flow rate of the fuel. This is due to the fact that a higher fuel inlet temperature would require less amount of heat to be produced in the combustor for the same turbine inlet temperature and therefore would reduce the fuel consumption rate in terms of mass of the fuel. Since thermal efficiency is the ratio of power output to the amount of combustion energy input, it would increase due to the reduction in the heat energy input for the same power developed.

Pinch point is defined as the temperature difference between the exhaust gases exiting from the evaporator of the HRSG and the saturation temperature of water exiting from the economizer. The pinch point is an important parameter for the design of HRSG and determines the cost of the heat exchanger. The higher the value of the pinch point, the smaller will be the heat transfer area required in the HRSG and hence, the lesser will be the initial investment cost of the HRSG and the whole plant [28]. Hence, this parameter needs to be selected very wisely. In the present study, the pinch point is varied from 5°C - 30°C. Fig. 6. clearly demonstrates that an increase in pinch point decreases the overall thermal efficiency of the CC. The reason for this behavior is that with an increase in the pinch point, the heat exchange between the flue gases and the water would reduce for the same heat transfer area. For this reason, the steam would absorb a lesser amount of flue gas heat and would attain a lower value of temperature and therefore, with less amount of heat input to the bottoming cycle, less power would be produced in the bottoming cycle and major portion of the flue gas heat would remain unused.

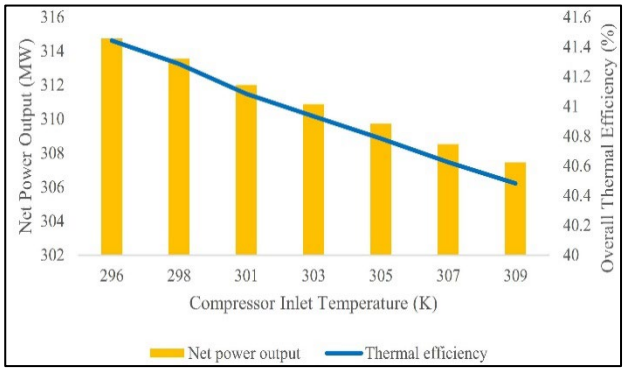

Fig. 4. Behavior of compressor inlet temperature on output parameters of the considered cycle.

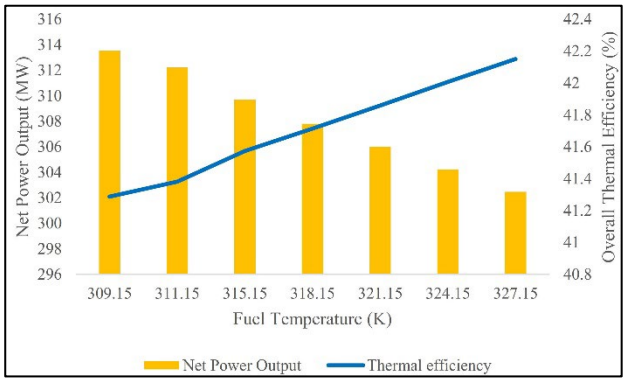

Fig. 5. Behavior of fuel temperature on output parameters of the considered cycle.

5. Conclusions

In this research work, the energetic and exergetic analysis of the above-mentioned plant is conducted through computer simulation in MATLAB to evaluate its performance and identify the components or places where major thermodynamic losses are taking place so that attention may be focused on those places or components to reduce the losses. The following conclusions are made in the proposed work:

- The simulated results of the power generated by the two gas turbine units (101.08 MW and 104.06 MW) and that of the steam turbine (110.795 MW) were found to match well with their actual values of 100.56 MW, 103.50, and 110 MW respectively. This validates the authenticity of the simulation model.
- The energy analysis revealed that around 8.27% of the combustion energy of fuel is wasted into the atmosphere along with the exhaust gases leaving the stack while 50.86% of combustion energy is discharged out to the cooling water in the condenser.
- However, the exergy analysis, revealed that the exergy content of exhaust gases is 11.2% while the exergy content of the heat lost in the condenser is only 1.39%. Due to higher exergy

content, the exhaust gases may be further utilized for generating additional power, while the condenser heat, which has low exergy content, can only be utilized in low temperature applications other than generating power.

- It is found that the combustor is the most irreversible component with the maximum percentage of exergy loss (14.9 % of the fuel exergy input) followed by stack (11.84 %), HRSG (11.72 %), steam turbine (7.74 %), and gas turbine (5.27 %). Therefore, maximum attention is needed to be centered on the combustors and efforts should be made and means to be developed to reduce this irreversibility thereby, increasing the power output of the plant.

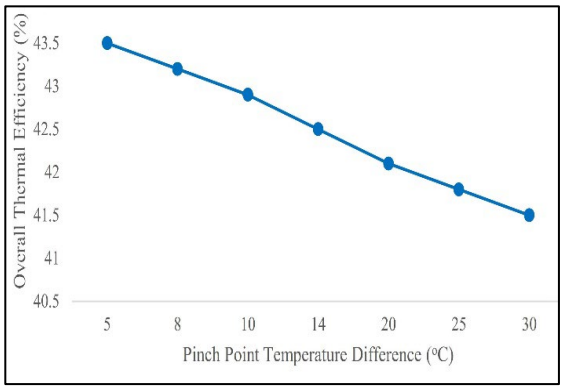

Fig. 6. Behavior of pinch point temperature difference on overall thermal efficiency.

Acknowledgements

The present study was supported by Indira Gandhi Delhi Technical University for Women under a financial grant scheme of 'IGDTUW Research Fellowship Scheme (JRF/SRF)'.

Nomenclature

$(A/F)_{mass}$	Air to Fuel ratio by mass
CCPP	Combined cycle power plants
CC	Combined cycle
$C_{p,i}$	Specific molar heat capacity (kJ/kmol-K)
CEP	Condensate extraction pump
CPH	Condensate preheater
GT 1	Gas Turbine cycle 1
GT 2	Gas Turbine cycle 2
HPBFW	High pressure boiler feed water
HP	High pressure
h	Specific enthalpy (kJ/kg)
HRSG	Heat recovery steam generator
$\hat{H}$	Total sensible enthalpy (kW)
LP	Low pressure
LPBFW	Low pressure boiler feed water
P	Pressure (kPa)
n	Number of moles (kg/kg-kmol)
$\hat{m}$	Rate of Mass flow (kg/s)
M	Molecular mass (kg/kmol)
$\hat{E}$	Energy generation rate (kJ/sec)
$\hat{E}_Q$	Energy flow due to heat (kJ/sec)
$\hat{E}_W$	Energy flow due to work (kJ/sec)
$\hat{X}$	Rate of total exergy flow(kJ/kmol)
$\hat{X}_D$	Exergy destruction rate (kJ/sec)
$\hat{X}_Q$	Exergy flow due to heat (kJ/sec)
$\hat{X}_W$	Exergy flow due to work (kJ/sec)
$\hat{P}$	Power produced(kW)
$\hat{W}$	Rate of work done (kW)
$\hat{Q}_i$	Rate of heat transfer(kW)
$\dot{n}$	molar flow rate (kmol/sec)
T	Temperature (K)
I^{st}	First law of thermodynamics
2^{nd}	Second Law of thermodynamics

Greek symbols

η	efficiency (–)
ψ	Rate of exergy flow (kJ/s)

Subscripts

in	Inlet
ex	Exit
a	Air
f	fuel
i	Number of components
0	Ambient condition
phy	Physical
ch	Chemical
tot	Total
HPST	High pressure steam turbine
LPST	Low pressure steam turbine
Dea	Deaerator
CA	Air compressor
GT	Gas turbine
Comb	Combustion chamber
ECC	Existing combined cycle
TC	Topping cycle
BC	Bottoming cycle
CON	Condenser

References

1) A. Wahid, D. R. Mustafida, and Y. A. Husnil, "Exergy Analysis of Coal-Fired Power Plants in

Ultra Supercritical Technology versus Integrated Gasification Combined Cycle," *Evergreen,* **7** *(1)* 32-42 (2020). https://doi.org/10.5109/2740939.

2) H. Gima, and T. Yoshitake, "A comparative study of energy security in okinawa prefecture and the state of Hawaii," *Evergreen: Joint Journal of Novel Carbon Resource Sciences and Green Asia Strategy,* **3** *(2)* 36-44 (2016). https://doi.org/10.5109/1800870
3) K. Uddin, I. El-Sharkawy, T. Miyazaki, B. B. Saha, and S. Koyama. "Thermodynamic Analysis of Adsorption Cooling Cycle using Ethanol-Surface treated Maxsorb III Pairs," *Evergreen*, **1** *(1)* 25-31 (2014). https://doi.org/10.5109/1440973
4) M. I. Alhamid, N. Nasruddin, Budihardjo, E. Susanto, T. F. Vickary, and M. A. Budiyanto, "Refrigeration cycle exergy-based analysis of hydrocarbon (R600a) refrigerant for optimization of household refrigerator," *Evergreen*, **6** *(1)* 71-77 (2019). https://doi.org/10.5109/2321015.
5) M. Purjam, K. Thu, and T. Miyazaki, "Thermodynamic Feasibility Evaluation of a Novel low temperature Ejector-based Trans-critical R744 Refrigeration Cycle," *Evergreen: Joint Journal of Novel Carbon Resource Sciences and Green Asia Stratergy,* **8** *(1)* 204-212 (2021). doi:10.5109/4372280.
6) Y. Gunawan, N Putra, E. Kusrini, I. Ibnu Hakim, and Md. D. H. Setiawan, "Study of Heat Pipe Utilizing Low-Temperature Geothermal Energy and Zeolite-A for Tea Leaves Withering Process," *Evergreen*, **7** *(2)* 221-227 (2020). https://doi.org/10.5109/4055223.
7) P. Pal, A. K. Nayak, and R. Dev, "A modified double-slope basin-type solar distiller: experimental and enviro-economic study," *Evergreen,* **5** *(1)* 52-61 (2018). https://doi.org/10.5109/1929730.
8) M. Khanam, Md. F. Hasan, T. Miyazaki, B. B. Saha, and S. Koyama, "Key factors of solar energy progress in Bangladesh until 2017," *Evergreen*, **5** *(2)* 78-85 (2018). https://doi.org/10.5109/1936220.
9) S. S. Mendu, P. Appikonda, and A. K. Emadabathuni, "Techno-Economic Comparative Analysis between Grid-Connected and Stand-Alone Integrated Energy Systems for an Educational Institute," *Evergreen*, **7** *(3)* 382-395 (2020). https://doi.org/10.5109/4068616.
10) M. Sharma, and R. Dev, "Review and Preliminary Analysis of Organic Rankine Cycle based on Turbine Inlet Temperature," *Evergreen,* **5** *(3)* 22-33 (2018).
11) S. C. Kaushik, V. S. Reddy, & S. K. Tyagi, "Energy and exergy analyses of thermal power plants: A review," *Renewable and Sustainable energy reviews*, **15** *(4)* 1857-1872 (2011). https://doi.org/10.1016/j.rser.2010.12.007
12) M. S. Ali, Q. N. Shafique, D. Kumar, S. Kumar, S. Kumar, "Energy and exergy analysis of a 747-MW combined cycle power plant Guddu," *International Journal of Ambient Energy*, **41** *(13)* 1495-1504 (2020). doi: 10.1080/01430750.2018.1517680.
13) A. Almutairi, P. Pilidis, N. Al-Mutawa, "Energetic and Exergetic Analysis of Combined Cycle Power Plant: Part-1 Operation and Performance," Energies, **8** *(12)* 14118-14135 (2015). https://doi.org/10.3390/EN81212418.
14) T. J. Kotas, "The exergy method of thermal plant analysis," Butterworths, London, 1985.
15) I. Dincer, M. A. Rosen, "Exergy: energy, environment and sustainable development," Newnes, 2012.
16) A. Cihan, O. Hacihafizoğlu, and K. Kahveci, "Energy-exergy analysis and modernization suggestions for a combined-cycle power plant," *International Journal of Energy Research*, **3** *(2)* 115–126 (2006). https://doi.org/10.1002/er.1133
17) T. K. Ibrahim, M. M. Rahman, and A. N. Abdalla, "Optimum gas turbine configuration for improving the performance of combined cycle power plant," *Procedia Engineering*, **15** 4216–4223 (2011). https://doi.org/10.1016/j.proeng.2011.08.791
18) M. Ameri, P. Ahmadi, S. Khanmohammadi, "Exergy analysis of a 420 MW combined cycle power plant," *International Journal of Energy Research*, **32** *(2)* 175–83 (2008). https://doi.org/10.1002/er.1351
19) E. Ersayin, & L. Ozgener, "Performance analysis of combined cycle power plants: A case study," *Renewable Sustainable Energy Reviews*, **43** 832–842 (2015). https://doi.org/10.1016/j.rser.2014.11.082.
20) M. Aliyu, A. B. AlQudaihi, S. A. M. Said, & Md. A. Habib, "Energy, exergy and parametric analysis of a combined cycle power plant," *Thermal Science and Engineering Progress*, **15** 100450 (2020). https://doi.org/10.1016/j.tsep.2019.100450
21) A. K. Shukla, O. Singh, "Effect of Compressor Inlet Temperature & Relative Humidity on Gas Turbine Cycle Performance," *International Journal of Scientific and Engineering Research*, **5** *(5)* 664-670 (2014).
22) M. N. Khan, I. Tlili, "Innovative thermodynamic parametric investigation of gas and steam bottoming cycles with heat exchanger and heat recovery steam generator: Energy and exergy analysis," *Energy Reports,* **4** 497–506 (2018). https://doi.org/10.1016/j.egyr.2018.07.007.
23) A. Khaliq, and S. C. Kaushik, "Second-law based thermodynamic analysis of Brayton/Rankine combined power cycle with reheat," *Applied. Energy*, **78** *(2)* 179–197 (2004). https://doi.org/10.1016/j.apenergy.2003.08.002
24) O. K. Singh and S. C. Kaushik, "Variables influencing the exergy based performance of a steam

power plant," *International Journal of Green Energy*, **10** *(3)* 257–284 (2013). https://doi.org/10.1080/15435075.2011.653847

25) Y. A. Çengel, and M. A. Boles, "Thermodynamics: An Engineering Approach 8th Edition in SI Units," McGraw Hill, 2015.
26) O. K. Singh, "Combustion simulation and emission control in natural gas fuelled combustor of gas turbine," *Journal of Thermal Analysis and Calorimetry*, **125** *(2)* 949-957 (2016). https://doi.org/10.1007/s10973-016-5472-0.
27) O. K. Singh, "Assessment of thermodynamic irreversibility in different zones of a heavy fuel oil fired high pressure boiler," *Journal of Thermal Analysis and Calorimetry,* **123** *829-840* (2016). https://doi.org/10.1007/s10973-015-4959-4.
28) S. F. Rezeka, W. M. El-maghalany, & A. M. Abdelhalim, "Influence of Pinch Point Temperature on the Performance of Integrated Solar Combined Cycle," *International Journal of Engineering Research and Technology*, **6** *(6)* 269-272 (2017).